On the Performance Degradation of GPS Positioning due to Outdated RT-PPP Products ⋆

Izadora A. Ramos * **Felipe O. Silva** * **Ludmila A. de Oliveira** *
Danilo A. de Lima * **Rogério P. Menezes Filho** ** **Jay A. Farrell** ***

* *Departamento de Automática, Universidade Federal de Lavras, MG, (e-mails: izadora.ramos@estudante.ufla.br, felipe.oliveira@ufla.br, ludmila.oliveira@estudante.ufla.br, danilo.delima@ufla.br)*
** *MWF Services Ltda., Departamento de Pesquisa e Desenvolvimento, (e-mail: rogerio.menezes@mwf-mechatronics.com)*
*** *Department of Electrical and Computer Engineering, University of California, Riverside, USA, (e-mail: farrell@ece.ucr.edu)*

Abstract: Real-time Precise Point Positioning (RT-PPP) is a technique that improves positioning accuracy by correcting common mode errors present in GNSS observables by means of products made available in real-time by specialized agencies, such as the International GNSS Service (IGS) and the Faculty of Astronomical and Geophysical Sciences (FCAG) of the Argentine University of La Plata (UNLP). The Real-Time Service (RTS) of IGS provides various correction streams for RT-PPP deployment, whose availability is beyond 95% for the Global Positioning System (GPS) and 90% for the GLObal NAvigation Satellite System (GLONASS). During the epochs the correction streams becomes momentarily unavailable or, when communication problems/latency occur, the equipment user has no other option than to use outdated products, which may degrade position accuracy. The objective of this work is to evaluate the impact of using outdated RT-PPP products on GPS positioning accuracy in Brazilian territory. As main contribution, we show that the RT-PPP GPS positioning accuracy is not significantly degraded when outdated products up to 25 minutes are used, being able to comply with the Society of Automotive Engineers (SAE) J2945 specification, which stipulates a maximum horizontal position error of 1.5 meter, at 68% of probability, aiming at Connected Autonomous Vehicle (CAV) applications. Results from experimental tests are conducted, in a stationary environment, which validates the outline verifications.

Keywords: GPS, RT-PPP, performance analysis, latency.

1. INTRODUCTION

Global Navigation Satellite Systems (GNSS) positioning is based on the transmission of signals from orbiting satellites, which provides three types of measurements: pseudorange (distance between the satellite and the receiver during the transmission and reception of the GNSS signal), Doppler shift (the relative velocity between the satellite and receiver), and carrier phase (distance between satellite and receiver expressed in cycles of the carrier wave). GNSS signals are affected by several sources of errors that affect GNSS positioning. Pseudorange measurements (the main GNSS observable and, hence, the one we focus on) are primarily corrupted by seven types of errors (Lachapelle, 1991; Teunissen, 1991), which can be classified into two categories (Farrell et al., 1996):

- *Common-mode errors* are spatially and temporally correlated errors, i.e, they are experienced similarly by all receivers in the same vicinity over short time spans. They comprise the ephemeris error, satellite clock bias, ionospheric and tropospheric delays;
- *Noncommon-mode errors* are different for each receiver even when separated by short distances, being comprised of receiver clock bias, multipath error, and receiver tracking noise.

A number of solutions are available to reduce the effect of common-mode errors on GNSS position estimation. In recent decades, Precise Point Positioning (PPP) and its Real-Time counterpart (RT-PPP) have emerged, and are constantly being improved (Grinter and Roberts, 2011; Gao and Chen, 2004). In traditional, i.e., post-processed PPP, for instance, the user equipment position is computed based on two-frequency pseudorange and carrier measurements in addition to precise corrections (also referred to as products) to the orbits and clocks of the tracked satellites. A breakthrough is taking place regarding the

⋆ This study was financed in part by the Research Development Foundation (FUNDEP - ROTA 2030), under grant 27192.02.02/2021.01.00, in part by the Brazilian Agricultural Research Corporation (EMBRAPA), under grant 212-20/2018, in part by the Brazilian National Council for Scientific and Technological Development (CNPq), under grants 313160/2019-8 and 312194/2022-6, in part by the Minas Gerais State Agency for Research and Development (FAPEMIG), under grants APQ-01449-17 and APQ-04659-22, and in part by the Postgraduate Support Program (PROAP), under grants 88881.708828/2022. The authors thank the Graduate Program on Systems Engineering and Automation (PPGESISA) of the Federal University of Lavras (UFLA) for supporting this work.

real-time availability of such corrections from the International GNSS Service (IGS), as well as the determination of integer ambiguities, in a few minutes, allowing the user to reach centimetric precision in real-time. RT-PPP with ambiguity solution has been named RT-PPPK (Wabbena et al., 2005; Teunissen and Khodabandeh, 2015). According to Krueger et al. (2020), the method has shown to be very promising, and the author states that the latter can be used with reference networks that are sparser than the Network Real-Time Kinematics (NRTK) approach. Hence, for users who need results comparable to traditional RTK (i.e. instantaneous solutions with $1 \sim 2$ cm error, using a nearby base station), the RT-PPPK method has been considered a complementary, lower-cost solution to serve regions where NRTK coverage is not available (Rovira-Garcia et al., 2015; Oliveira Junior, 2017).

A main drawback of RT-PPPK, as is also the case for RTK and NRTK, is that the associated ambiguity resolution problem is not easily solved unless two-frequency GNSS measurements are employed (Verhagen et al., 2012). As the cost of GNSS two-frequency user equipment is much higher than its single-frequency counterpart, the employment of such techniques may be prohibitive, especially for mass-market applications. In this regard, many works have devoted time to investigate the performance capabilities of RT-PPP exclusively for pseudorange-based single-frequency users (Bahadur and Nohutcu, 2020; Rahman et al., 2022), as is the case of this work.

In RT-PPP applications, the availability and latency of products delivered to users are of paramount importance. Lack of correction data eliminates satellites from position computation, and obsolete products may introduce errors whose magnitude may increase with latency. Both factors may significantly degrade GNSS estimation performance. To investigate the availability of RT-PPP products, Hadas and Bosy (2015) employed the BKG Ntrip Client (BNC) software and showed the corrections provided by IGS have an average availability of 92% for GPS and GLObal NAtigation Satellite System (GLONASS) satellites. Further aiming at evaluating the impact of interrupting communication to obtain RT-PPP positioning corrections using only IGS orbit and clock products, the authors concluded that, on average, an additional position error of 5 cm is expected when using orbit corrections with 3 minutes of latency and clock correction with 1 of minute latency.

IGS currently provides RT-PPP corrections with global coverage for the most important remaining common-mode errors: GPS/GLONASS satellite orbit, clock and hardware bias; and, ionospheric delay. In addition, regional agencies have recently succeed in establishing correction services to better serve their local users. For example, Silva et al. (2023) showed that for Connected Autonomous Vehicle (CAV) applications in Brazilian territory, the ionospheric products broadcast by the Faculty of Astronomical and Geophysical Sciences (FCAG) of the Argentine University of La Plata (UNLP) attained superior performance relative to the standard ionospheric corrections provided by the IGS. For this product, however, a small latency exists that is stated to be lower than 10 minutes. (Mendoza et al., 2019a)

Thus, the objective of this work is to investigate the performance degradation of currently available RT-PPP solutions as a function of the obsolescence/latency of the corresponding corrections with a focus on CAV applications in Brazilian territory. As main contribution, we show that the RT-PPP GPS positioning accuracy is not significantly degraded when outdated products up to 25 minutes are used, being able to comply with the Society of Automotive Engineers (SAE) J2945 specification, which stipulates a maximum horizontal position error of 1.5 meter, at 68% of probability, aiming at Connected Autonomous Vehicle (CAV) applications (SAE, 2016).

The remainder of this work is organized as follows: Section 2 introduces the notation and background for RT-PPP position estimation using Single-Frequency (SF) pseudorange measurements. Section 3 describes experimental data and discusses positioning performance of SF GPS-based RT-PPP when outdated products are used. Section 4, lastly, summarizes the paper and presents final thoughts and conclusions.

2. RT-PPP BACKGROUND

The pseudorange measurement between a user antenna a and a satellite s, taking into account the errors cited in Section 1, can be modeled as:

$$\rho^s_{a,R} = r_{as} + \delta\rho^a_c - \delta\rho^s_c + \delta\rho^s_{I,a} + \delta\rho^s_{T,a} + \delta\rho^s_E + \delta\rho^s_{M,a} + w^s_{p,a}, \quad (1)$$

where the true range r_{as} between ECEF user position $\mathbf{r}^e_{ea}$ and ECEF satellite position $\mathbf{r}^e_{es}$ is defined as:

$$r_{as} = \left| \mathbf{C}^I_e \, \mathbf{r}^e_{es} - \mathbf{r}^e_{ea} \right|. \quad (2)$$

The symbol $\mathbf{C}^I_e$ represents the Direct Cosine Matrix (DCM) compensating for ECEF rotation during signal propagation, for more details see section 2.4.1 from Farrell (2008). In (2), the superscript e indicates that position is measured with respect to the Earth-Centered-Earth-Fixed (ECEF) frame. In (1), $\delta\rho^a_c$ represents the receiver clock bias, $\delta\rho^s_c$ is the satellite clock bias, $\delta\rho^s_{I,a}$ is the ionospheric delay, $\delta\rho^s_{T,a}$ is the tropospheric delay, $\delta\rho^s_E$ is the ephemeris error, $\delta\rho^s_{M,a}$ is the multipath error, and $w^s_{p,a}$ is the receiver tracking noise.

The parameter of interest in the estimation problem of (1)-(2) is generally the user position, whose functional relationship to the pseudorange measurement is nonlinear. Example methods to estimate position are Weighted Iterated Least Squares (WILS) or the Extended Kalman Filter (EKF). Such estimation methods are beyond the scope of this article. The interested reader is referred to (He et al., 2010; Farrell, 2008) for additional information.

2.1 RT-PPP Implementation

Traditional PPP has been post-processed due to the latency involved with the generation of precise orbit and clock products. There is an inherent tradeoff between latency and accuracy. In RT-PPP, IGS Analysis Centers (ACs) provide slightly less accurate (w.r.t. final products) real-time orbit and clock corrections formatted according to the Radio Technical Commission for Maritime Services (RTCM) 10,403.x protocols. These corrections are broadcasted to global users by means of Networked Transport of

RTCM via Internet Protocol (NTRIP) with low latency. The format of the real-time products and the usage of NTRIP are discussed in (Li et al., 2022).

The IGS State Space Representation (SSR) format is an open standard for the dissemination of real-time products to support the IGS RTS and the wider community. The messages support multi-GNSS and include corrections for satellite orbits, clocks, Differential Code Biases (DCBs), phase-biases, and ionospheric delays. The principle of SSR is to provide information to model individual error sources acting on GNSS to enable improved positioning for the user (IGS, 2023). In general, the continuous chronology of messages can be used to check for their consistency, but in real-time applications, messages may be lost or delayed. A consistency parameter is also the GNSS specific Issue of Data (IOD), which can be used to check for the appropriateness of applying SSR orbit and clock corrections.

IGS SSR Satellite Orbit Correction The SSR orbit correction message contains the parameter for orbit correction $\delta\mathbf{O}$ in the radial, along-track, and cross-track components. These are used to compute a satellite position correction $\delta\mathbf{r}$, to be applied to the satellite position $\mathbf{r}^e_{es,B}$ calculated according to corresponding GNSS Interface Control Document (ICD) from the broadcast ephemeris parameter set identified by the GNSS IOD in SSR orbit correction message. The sign definition of the correction is:

$$\mathbf{r}^e_{es,C} = \mathbf{r}^e_{es,B} + \delta\mathbf{r}, \tag{3}$$

where $\mathbf{r}^e_{es,C}$ is the satellite position vector corrected by the SSR orbit correction message. The satellite position correction $\delta\mathbf{r}$ is computed according to:

$$\delta\mathbf{r} = [e_{radial} \;\; e_{cross} \;\; e_{along}]\delta\mathbf{O}, \tag{4}$$

where:

$$\begin{aligned} e_{along} &= \frac{\dot{\mathbf{r}}^e_{es,B}}{\mathbf{r}^e_{es,B}} \\ e_{cross} &= \frac{\mathbf{r}^e_{es,B} \times \dot{\mathbf{r}}^e_{es,B}}{\left|\mathbf{r}^e_{es,B} \times \dot{\mathbf{r}}^e_{es,B}\right|}. \\ e_{radial} &= e_{along} \times e_{cross} \end{aligned}$$

The complete orbit correction vector $\delta\mathbf{O}$ is computed from the individual correction terms and their rates:

$$\delta\mathbf{O} = \begin{bmatrix} \delta\mathbf{O}_{radial} \\ \delta\mathbf{O}_{along} \\ \delta\mathbf{O}_{cross} \end{bmatrix} + \begin{bmatrix} \delta\dot{\mathbf{O}}_{radial} \\ \delta\dot{\mathbf{O}}_{along} \\ \delta\dot{\mathbf{O}}_{cross} \end{bmatrix} (t - t_0). \tag{5}$$

where t is the GNSS time of transmission and t_0 is the reference time obtained from the SSR orbit correction message. After correcting $\mathbf{r}^e_{es,C}$ as shown in (3), the residual ephemeris error $\delta\rho^s_E$ remaining on the model of (1) is considered to be negligible.

IGS SSR Satellite Clock Correction The SSR clock correction message contains the parameters to compute the polynomial clock correction δC that should be applied to the broadcast satellite clock. The sign definition of the corrections is:

$$t_{st,C} = t_{st,B} - \frac{\delta C}{c}, \tag{6}$$

where c is the speed of light, $t_{st,B}$ is the satellite time of transmission computed according to the GNSS ICD from broadcast clock parameters, identified by the GNSS IOD of the corresponding SSR clock correction message, and $t_{st,C}$ is the corrected satellite time. The polynomial correction is computed according to:

$$\delta C = C_0 + C_1(t - t_0) + C_2(t - t_0)^2, \tag{7}$$

where $C_i, i = 0, 1, 2$ are the polynomial coefficients from the SSR clock correction message.

IGS SSR Satellite Bias Correction Hardware delays, either at the satellite or at the receiver, are caused by the difference between the paths taken by the carriers (L1 and L2, from GPS, for example) in the hardware. These delays are not directly accessible in their absolute form, as they are obtained only when combining carriers. For this reason, such delays or biases are often referred to as Differential Code Biases (DCB). DCB based on IGS RT products is calculated as follows:

$$DCB = \frac{C1W - C1C}{c} \tag{8}$$

where C1W and C1C are the Precise (P) and Coarse Acquisition (C/A) GPS code bias on frequency L1 provided by the IGS products. Based on (8), a refined (subscript R) version of the satellite clock correction δC defined in (7) can be formed as:

$$\delta C_R = \delta C + DCB \tag{9}$$

which is to be used in place of δC in (6). After correcting $t_{st,C}$ as suggested, the residual satellite clock error $\delta\rho^s_c$ remaining on the model of (1) is considered to be negligible.

2.2 FCAG-UNLP Ionosphere Correction

To enable greater accuracy over South America, Caribbean, and Antarctic peninsula, FCAG-UNLP recently started producing its own RT-PPP ionospheric products, in the form of single-layer Vertical Total Electron Content (VTEC) maps, based on a regional network of GNSS Continuously Operating Reference Stations (CORS) (Mendoza et al., 2019a,b). Model data is provided in the IONosphere EXchange (IONEX) format (regularly used by IGS to convey its final ionospheric products) with an update period of 15 minutes.

FCAG-UNLP directly provides estimated $VTEC_{j,k}$ values on an equidistant grid with 0.5 degrees resolution for geocentric latitude L_j and longitude λ_k. Application of the single-layer model, however, requires interpolation for the so-called Ionosphere Pierce Point (IPP) position location (λ_{IPP}, L_{IPP}). As suggested by Teunissen and Montenbruck (2017), a suitable interpolation technique is the bilinear one, according to that the VTEC value at the IPP coordinates is computed as:

$$\begin{aligned} VTEC(\lambda_{IPP}, L_{IPP]}) = (1-p)(1-q)VTEC_{j,k} + \\ (p)(1-q)VTEC_{j+1,k} + \\ (1-p)(q)VTEC_{j,k+1} + \\ (p)(q)VTEC_{j+1,k+1} \end{aligned}, \tag{10}$$

where:

$$\begin{aligned} p &= (L_{IPP} - L_j)/(L_{j+1} - L_j) \\ q &= (\lambda_{IPP} - \lambda_k)/(\lambda_{k+1} - \lambda_k), \end{aligned} \tag{11}$$

which is applied in the intervals $L_j \leq L_{IPP} \leq L_{j+1}$ and $\lambda_k \leq \lambda_{IPP} \leq \lambda_{k+1}$, bounded by the surrounding grid points.

To compute the Slant TEC (STEC) contribution of the layer, it suffices doing (Nie et al., 2019):

$$STEC = \frac{VTEC}{sin(E + \lambda_{PP})} \tag{12}$$

where E is the elevation angle of the satellite with respect to the user location. The ionospheric correction $\delta\rho^s_{I,a}$, to be used for compensating the model (1), can be estimated, in meters and for the specific frequency f, as:

$$\delta\hat{\rho}^s_{I,a} = \frac{40.3}{f^2} 10^{16} STEC \tag{13}$$

2.3 Empirical Tropospheric Correction

Corrections for tropospheric delays are the sole RT-PPP products that are not currently provided by any specialized agency. They are foreseen though, for the third stage of IGS-RTS deployment (IGS, 2020). At present, worldwide RT-PPP users have to rely on predetermined empirical models of the tropospheric delays that take into account typical seasonal variations of atmospheric parameters, e.g., temperature, pressure, relative humidity, etc. as a function of location. A recent investigation by de Oliveira et al. (2023) showed that among several state-of-the-art tropospheric models described in the literature, the one proposed by the University of New Brunswick (UNB3) performed best in Brazilian territory, even in comparison with its more recent and modified version UNB3m (Leandro et al., 2006).

In the UNB3 troposphere delay model, the pressure, p, temperature, T, water vapor pressure, e, rate of change of temperature, β, and rate of change of water vapor, λ, are all predicted as a function of the user latitude, L_a, and day of year, d, using:

$$\begin{aligned} p &= p_0(L_a) + p_\sigma(L_a) cos[2\pi(d - d_{min})/365, 25] \\ T &= T_0(L_a) + T_\sigma(L_a) cos[2\pi(d - d_{min})/365, 25] \\ e &= e_0(L_a) + e_\sigma(L_a) cos[2\pi(d - d_{min})/365, 25] \\ \beta &= \beta_0(L_a) + \beta_\sigma(L_a) cos[2\pi(d - d_{min})/365, 25] \\ \lambda &= \lambda_0(L_a) + \lambda_\sigma(L_a) cos[2\pi(d - d_{min})/365, 25] \end{aligned} \tag{14}$$

where the subscript 0 denotes the mean value, the subscript σ denotes the amplitude of the seasonal variation, and d_{min} is 28 in the northern hemisphere and 211 in the southern hemisphere. The UNB3 model provides values for each quantity. The dry (subscript d) and wet (subscript w) tropospheric zenith (subscrit Z) delays are then calculated using:

$$\delta\hat{\rho}_{TZd} = \left(1 - \frac{\beta H_a}{T}\right)^{\frac{g}{R_d\beta}} \left(\frac{k_1 R_d p}{g_m}\right), \tag{15}$$

$$\delta\hat{\rho}_{TZw} = \left(1 - \frac{\beta H_a}{T}\right)^{\frac{(\lambda+1)g}{R_d\beta}} \left(\frac{k_2 R_d pe}{[g_m(\lambda+1) - \beta R_d]T}\right), \tag{16}$$

where H_a is the receiver orthometric altitude, and g, R_d, k_1, g_m, and k_2 are constants defined in (Leandro et al., 2006). Finally, the slant troposphere propagation delay for each individual signal is estimated using:

$$\delta\hat{\rho}^s_{T,a} = m_d\, \delta\hat{\rho}_{TZd} + m_w\, \delta\hat{\rho}_{TZw} \tag{17}$$

where m_d and m_w are Niell dry and wet mapping functions, respectively (Niell, 1996).

3. EXPERIMENTAL RESULTS

This Section presents the results of stationary experimental tests intended to evaluate the RT-PPP GPS performance degradation in the event of only outdated products from IGS and FCAG-UNLP being available. The idea was to simulate a scenario (likely to occur in real applications) characterized by the interruption of RT-PPP streams on BNC, and/or the existence of excessive latency on the generation of the latter, or yet, an eventual loss of internet connection by the user.

In the conducted experiments, we focused on SF pseudorange measurements from the GPS constellation and on ionospheric products from FCAG-UNLP. All other RT-PPP products were obtained from IGS by its RTS. Tropospheric corrections were computed following UNB3 empirical model.

3.1 Experimental Data Acquisition and Methodology

The expectation is that the accuracy of the RT-PPP corrections will deteriorate as the latency increases. To investigate this relation, the following experiment was carried out: we collected approximately 12 hours of GPS raw data (L1 C/A pseudorange measurements and navigation messages) in Receiver INdependent EXchange (RINEX) format from the static reference station designated as MGLA, which belongs to the Brazilian Network for Continuous Monitoring (RBMC) of GNSS, and is located at the Federal University of Lavras (UFLA). MGLA is equipped with a high-quality Trimble NETR9 receiver and a Zephyr 3 Geodetic (TRM115000.00) antenna. At the same time, we used BNC software to collect the SSR RT-PPP products from IGS-RTS, namely, the SSRA02IGS1 stream, which is an IGS Kalman filter combination solution conveying satellite orbit, clock and bias corrections. Lastly, we collected the near real-time UNLP-FCAG VTEC products directly from their File Transfer Protocol (FTP) server in IONEX format (Mendoza et al., 2019a,b). The whole test was conducted twice, the first starting on November 6, 2022 at 12:00 pm, and the second starting on March 16, 2023 at 12:40 pm.

After the data were collected, they were parsed and processed offline, using specialized MATLAB algorithms, developed by the authors, that employ a Weighted Iterated Least Squares (WILS) strategy for computing the RT-PPP position solution (for further details see Section 5.3.2 of Farrell (2008)). The errors were computed with respect to the ground truth position of MGLA, which is known to centimeter accuracy, as it is static and frequently surveyed by specialized personnel from the Brazilian Institute of Geography and Statistics (IBGE).

The following were the updated rates of the collected data: (a) 15 seconds for the GPS observables from MGLA; (b) 10 seconds for the IGS clock corrections; (c) 60 seconds for the IGS orbit and bias corrections; and (d) 15 minutes for the FCAG-UNLP ionospheric corrections. In order to evaluate the effects of obsolescence in these products and/or latency in communication, complete cycles of our RT-PPP algorithm were executed, with simulated obsolescences/latencies ranging from 0 to 1800 seconds at the step of 15 seconds per simulation, i.e., the RT-

PPP corrections used for executing the scripts were those obtained considering as if the Time of Week (TOW) of the GPS observables were the current ones subtracted from the obsolescence/latency value purposely inserted in the respective test cycle, i.e:

$$TOW_{cor} = TOW_{obs} - latency \tag{18}$$

where subscripts *cor* and *obs* stand for correction and observable, respectively.

To evaluate the performance degradation of the RT-PPP position estimation when outdated products were used, we established as a suitable metric, the horizontal Cartesian position error of the user, which is defined as:

$$\delta r^e_{ea,H} = \sqrt{(\delta r^e_{ea,N})^2 + (\delta r^e_{ea,E})^2} \tag{19}$$

where $\delta r^e_{ea,N}$ and $\delta r^e_{ea,E}$ are the North (subscript N) and East (subscript E) components of the user Cartesian position error, respectively.

We mainly focused on the horizontal position errors in this work, as these are the most important metrics for CAV applications. This can be inferred from: (a) the more strict accuracy constraints imposed by the SAE J2945 standard to the horizontal channel of vehicles (errors of 1.5 meter at 68% of probability), in comparison to the vertical channel (errors of 3.0 meters at the same probability); (b) the recent study by Williams and Barth (2020), who defines the required lane-level positioning accuracy for CAV applications as a function only of the horizontal positioning; and (c) the fact that CAV models for control and guidance purposes generally rely solely on the horizontal dynamics of the vehicle. For details, see Claussmann et al. (2019).

3.2 RT-PPP Performance Analysis

The results obtained for each test are presented in sequence. Figure 3.2 shows the graph of the Cumulative Distribution Function (CDF) obtained for Test 1, in terms of positioning error in the horizontal channel, considering obsolescences/latencies on the RT-PPP products ranging from 0 to 1800 seconds. It is possible to observe the gradual degradation of the positioning accuracy with the increase of the obsolescence/latency of the corrections. In Figure 3.2, the same trend can be observed for the results obtained for Test 2. The degradation of position accuracy with respect to RT-PPP product latency is an expected behavior due to the temporal correlation of the common mode errors. The main purpose of this work is to evaluate the maximum RT-PPP product latency that allows a sufficiently accurate cancellation of common mode errors for CAV purposes.

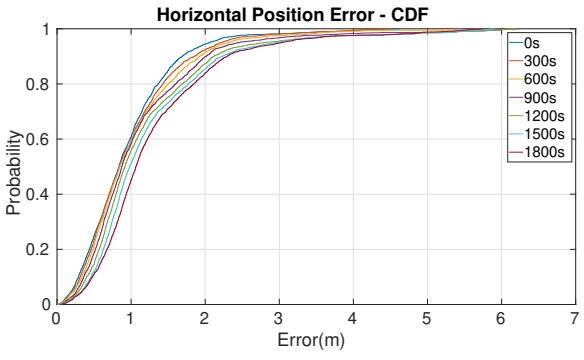

Figure 1. Horizontal position error CDF for Test 1

Tables 1 and 2 summarize position accuracy measures of the horizontal position errors for the investigated range of RT-PPP product latency. Column 1 shows the obsolescence/latency in seconds; column 2 shows the mean error; column 3 displays the STandard Deviation (STD); column 4 reports the maximum value for horizontal position error; and columns 5, 6, and 7 report the percent of samples that have horizontal position error less than 0.5 m, 1 m and 1.5 m, respectively. Figures 3.2 to 3.2 plot some of the accuracy measures above as a function of the obsolescence/latency of the RT-PPP products.

As can be seen in both Tables and Figures, the mean, standard deviation, and maximum values of the horizontal position errors show a gradual increase as the obsolescence/latency of the RT-PPP products is increased. The

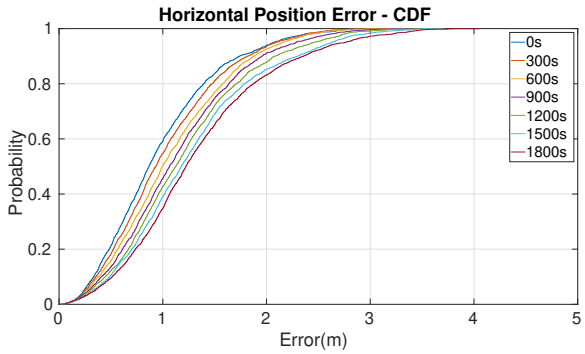

Figure 2. Horizontal position error CDF for Test 2

Table 1. Horizontal position performance for test 1.

Latency (s)	Mean (m)	Std. Dev.(m)	Max (m)	Probability (%)		
				<0,5 m	<1 m	<1,5 m
0	0.953	0.648	4.623	25.0	60.7	85.0
30	0.956	0.649	4.626	24.8	60.6	84.5
60	0.960	0.652	4.622	24.8	60.1	84.3
150	0.967	0.659	4.632	24.9	59.8	83.9
300	0.984	0.672	4.649	24.4	59.6	83.0
600	1.016	0.718	6.215	22.3	59.5	80.9
900	1.106	0.864	6.220	18.6	58.3	77.6
1200	1.120	0.928	6.207	18.4	58.2	77.3
1500	1.249	0.922	5.913	11.9	51.1	73.1
1800	1.308	0.908	5.761	11.0	45.1	71.0

Table 2. Horizontal position performance for test 2.

Latency (s)	Mean (m)	Std. Dev.(m)	Max (m)	Probability (%)		
				<0,5 m	<1 m	<1,5 m
0	0.967	0.557	3.164	21.3	59.2	83.8
30	0.973	0.558	3.300	20.8	58.4	83.4
60	0.978	0.557	3.296	20.6	58.3	83.2
150	0.993	0.556	3.321	19.7	56.5	82.6
300	1.020	0.561	3.316	18.2	54.8	81.1
600	1.082	0.576	3.342	15.8	50.3	77.0
900	1.142	0.603	3.402	13.7	45.7	74.8
1200	1.206	0.638	3.709	12.2	42.7	72.1
1500	1.278	0.681	3.698	10.5	39.1	69.0
1800	1.337	0.712	4.049	9.5	34.8	65.0

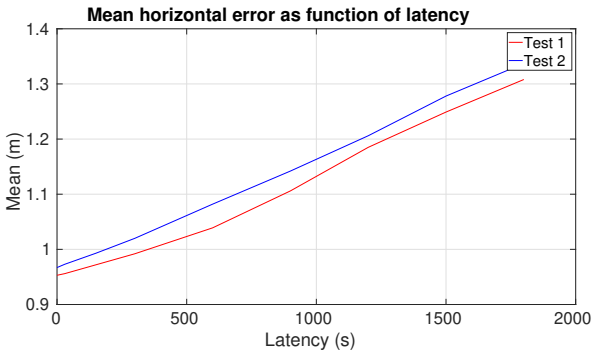

Figure 3. Mean horizontal error as function of latency

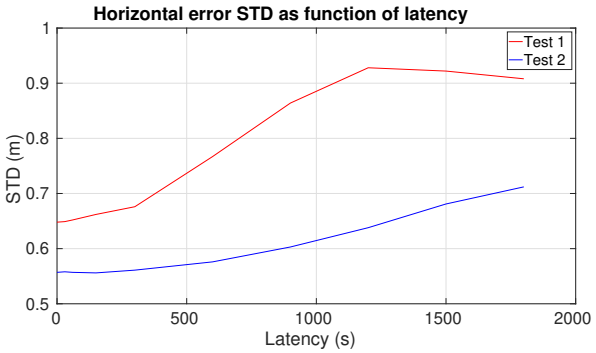

Figure 4. Horizontal error STD as function of latency

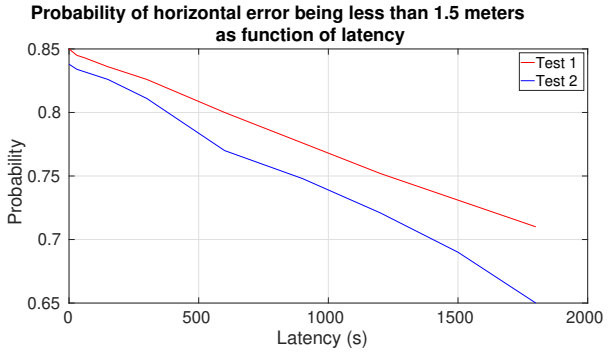

Figure 5. Probability of horizontal error being less than 1.5 meters as function of latency

percentage of samples with errors less than 0.5, 1.0, and 1.5 meter also decrease as latency increases. For the maximum considered latency of 1800 seconds, i.e., 30 minutes, we can observe that the percentage of samples with horizontal position error below 1.5 meter is 71% for Test 1 and 65% for Test 2. The SAE J2945 standard specifies that the required accuracy for the horizontal position for CAV applications is of 1.5 meters at 68%. In Test 1, the SAE specification is met for latency up to 1800 seconds. In Test 2, the SAE specification is met for latency up to 1500 seconds, i.e., 25 minutes. In a study conducted by Hadas and Bosy (2015) on the impact of purposely interrupting communication to simulate the usage of outdated IGS orbit and clock corrections for RT-PPP, they concluded that, on average, an additional error of 5 cm is expected to arise when using obsolete orbit and clock corrections by 3 minutes and 1 minute, respectively. Differently from Hadas and Bosy (2015), in this work, we employed IGS satellite orbit, clock, and bias products, in addition to FCAG-UNLP high-precision ionospheric corrections for South America, and the results showed that to achieve the same level of position degradation as in Hadas and Bosy (2015), i.e., of 5 cm, current RT-PPP products may be obsolete up to around 6 minutes. It is worth noting, however, that, in addition to the fact that Hadas and Bosy (2015) employed fewer RT-PPP products than us, their work was conducted in 2013, which allows us to infer the evolution of IGS product quality in the last years.

These results reaffirm the robustness of the RT-PPP position estimation approach when dealing with the effects of communication latency on the products, the event of loss of internet connection by the user, and/or the unavoidable interruption of the correction streams from the servers (IGS and FCAG-UNLP).

4. CONCLUSIONS AND FUTURE WORK

Accuracy in position estimation is of great interest in many commercial applications. This work investigated the performance degradation of currently available RT-PPP solutions as a function of the obsolescence/latency of the corresponding corrections with a focus on CAV applications in Brazilian territory. Results of experimental tests in a stationary environment showed that the RT-PPP positioning does not suffer a significant decrease in accuracy, i.e., it is smaller than 5 cm, for outdated products up to around 6 minutes. Additionally, we showed that RT-PPP is able to comply with the horizontal position constraints defined by the SAE J2945 standard provided the corresponding corrections were generated in the last 25 minutes. It is important to emphasize that the experiment described herein employed stationary high-performance receivers from RBMC. As the common-mode errors (which are the errors RT-PPP proposes to mitigate) are expected to be the same for GNSS receivers in the same vicinity, regardless of their quality, the results presented herein should extend, without loss of generality, to stationary low-cost receivers. As suggestions for future work, the authors intend to extend the same investigation to moving platforms equipped with low-cost, multi-constellations GNSS equipment.

REFERENCES

Bahadur, B. and Nohutcu, M. (2020). Real-time single-frequency multi-GNSS positioning with ultra-rapid products. *MEAS SCI TECHNOL*, 32(1), 014003.

Claussmann, L., Revilloud, M., Gruyer, D., and Glaser, S. (2019). A review of motion planning for highway autonomous driving. *IEEE T INTELL TRANSP*, 21(5), 1826–1848.

de Oliveira, L.A., Ramos, I.A., Silva, F.O., and de Lima, D.A. (2023). Comparative analysis between tropospheric models for GNSS positioning in Brazilian territory. *Proc. ABCM DINAME*, 37387, 1–10.

Farrell, J., Grewal, M., Djodot, M., and Barth, M. (1996). Differential GPS with latency compensation for autonomous navigation. In *Proceedings of the 1996 IEEE INT SYMP INTELL*, 20–24. IEEE.

Farrell, J. (2008). *Aided Navigation: GPS with High Rate Sensors*. McGraw-Hill, Inc.

Gao, Y. and Chen, K. (2004). Performance analysis of precise point positioning using real-time orbit and clock

products. *Journal of Global Positioning Systems*, 3(1-2), 95–100.

Grinter, T. and Roberts, C. (2011). Precise point positioning: where are we now. In *IGNSS Symposium*, 15–17.

Hadas, T. and Bosy, J. (2015). IGS RTS precise orbits and clocks verification and quality degradation over time. *GPS SOLUT*, 19, 93–105.

He, Y., Martin, R., and Bilgic, A.M. (2010). Approximate iterative Least Squares algorithms for GPS positioning. In *The 10th IEEE International Symposium on Signal Processing and Information Technology*, 231–236. IEEE.

IGS (2020). IGS state space representation (SSR) format version 1.00.

IGS (2023). IGS, International GNSS Service. URL `https://www.igs.gov/`. Acessed in: february / 2023.

Krueger, C.P., de Oliveira Junior, P.S., dos Anjos Garnés, S.J., Alves, D., and Euriques, J. (2020). Posicionamento GNSS em Tempo Real: Evolução, Aplicações Práticas e Perspectivas para o Futuro. *RBC*, 72, 1359–1379.

Lachapelle, G. (1991). GPS observables and error sources for kinematic positioning. In *Kinematic Systems in Geodesy, Surveying, and Remote Sensing*, 17–26. Springer.

Leandro, R., Santos, M., and Langley, R.B. (2006). UNB neutral atmosphere models: development and performance. *Proc. of ION NTM*, 52(1), 564–573.

Li, B., Ge, H., Bu, Y., Zheng, Y., and Yuan, L. (2022). Comprehensive assessment of real-time precise products from IGS analysis centers. *SPAC STUD*, 3(1), 12.

Mendoza, L.P.O., Meza, A.M., and Aragón Paz, J.M. (2019a). A multi-GNSS, multi-frequency and near real-time ionospheric TEC monitoring system for South America. *J SPACE WEATHER SPAC*, 17(5), 654–661.

Mendoza, L.P.O., Meza, A.M., and Aragón Paz, J.M. (2019b). Technical note on the multi-GNSS, multi-frequency and near real-time ionospheric TEC monitoring system for South America. *EarthArXiv*, 1–11. doi:10.31223/osf.io/3vts6.

Nie, Z., Yang, H., Zhou, P., Gao, Y., and Wang, Z. (2019). Quality assessment of CNES real-time ionospheric products. *GPS SOLUT*, 23, 1–15.

Niell, A.E. (1996). Global Mapping Functions for the Atmosphere Delay at Radio Wavelengths. *J. Geophys. Res.*, 101(B2), 3227–3246.

Oliveira Junior, P.S.d. (2017). Definition and implementation of a new service for precise GNSS positioning.

Rahman, F., Silva, F.O., Jiang, Z., and Farrell, J.A. (2022). Low-cost real-time ppp gnss aided ins for cav applications. *IEEE T INTELL TRANSP*, 23(12), 25018–25032.

Rovira-Garcia, A., Juan, J.M., Sanz, J., and Gonzalez-Casado, G. (2015). A worldwide ionospheric model for fast precise point positioning. *IEEE T GEOSCI REMOTE*, 53(8), 4596–4604.

SAE (2016). On-Board System Requirements for V2V Safety Communications. *SAE J2945/1*.

Silva, F.O., W., H., and Farrell, J.A. (2023). Real-Time Single-Frequency Precise Point Positioning for Connected Autonomous Vehicles: A Case Study over Brazilian Territory. *World Congress*.

Teunissen, P. (1991). Differential GPS: Concepts and quality control. *J INST NAVIG*, 10, 48–60.

Teunissen, P. and Montenbruck, O. (2017). *Handbook of Global Navigation Satellite Systems*. Springer International Publishing.

Teunissen, P. and Khodabandeh, A. (2015). Review and principles of PPP-RTK methods. *J GEODESY*, 89(3), 217–240.

Verhagen, S., Teunissen, P.J.G., and Odijk, D. (2012). The future of single-frequency integer ambiguity resolution. *VII Hotine-Marussi Symp. on Mathematical Geodesy, IAG SYMP 137*.

Wabbena, G., Schmitz, M., and Bagge, A. (2005). PPP-RTK: precise point positioning using state-space representation in RTK networks. In *Proceedings of the 18th international technical meeting of the satellite division of the Institute of navigation (ION GNSS 2005)*, 2584–2594.

Williams, N. and Barth, M. (2020). A qualitative analysis of vehicle positioning requirements for connected vehicle applications. *IEEE T INTELL TRANSP*, 13(1), 225–242.